INAF
ISTITUTO NAZIONALE
DI ASTROFISICA
NATIONAL INSTITUTE
FOR ASTROPHYSICS

Publication Year	2018
Acceptance in OA	2020-11-12T11:13:56Z
Title	GASP. IX. Jellyfish galaxies in phase-space: an orbital study of intense ram-pressure stripping in clusters
Authors	Jaffé, Yara L., POGGIANTI, Bianca Maria, MORETTI, ALESSIA, GULLIEUSZIK, MARCO, Smith, Rory, Vulcani, Benedetta, FASANO, Giovanni, Fritz, Jacopo, Tonnesen, Stephanie, BETTONI, Daniela, Hau, George, BIVIANO, ANDREA, BELLHOUSE, CALLUM, McGee, Sean
Publisher's version (DOI)	10.1093/mnras/sty500
Handle	http://hdl.handle.net/20.500.12386/28286
Journal	MONTHLY NOTICES OF THE ROYAL ASTRONOMICAL SOCIETY
Volume	476

Monthly Notices
of the
ROYAL ASTRONOMICAL SOCIETY

MNRAS **476,** 4753–4764 (2018)
Advance Access publication 2018 February 23

doi:10.1093/mnras/sty500

GASP. IX. Jellyfish galaxies in phase-space: an orbital study of intense ram-pressure stripping in clusters

Yara L. Jaffé,[1,2]★ Bianca M. Poggianti,[3] Alessia Moretti,[3] Marco Gullieuszik,[3] Rory Smith,[4] Benedetta Vulcani,[3,5] Giovanni Fasano,[3] Jacopo Fritz,[6] Stephanie Tonnesen,[7] Daniela Bettoni,[3] George Hau,[1] Andrea Biviano,[8] Callum Bellhouse[9] and Sean McGee[9]

[1]*European Southern Observatory, Alonso de Cordova 3107, Vitacura, Casilla 19001, Santiago de Chile, Chile*
[2]*Instituto de Física y Astronomía, Universidad de Valparaíso, Avda. Gran Bretaña 1111 Valparaíso, Chile*
[3]*INAF-Astronomical Observatory of Padova, vicolo dell'Osservatorio 5, I-35122 Padova, Italy*
[4]*Korea Astronomy and Space Science Institute, 766, Daedeokdae-ro, Yuseon-gu, Daejon, 34055, Korea*
[5]*School of Physics, The University of Melbourne, VIC 3010, Australia*
[6]*Instituto de Radioastronomí a y Astrofí sica, UNAM, Campus Morelia, A.P. 3-72, C.P. 58089, Mexico*
[7]*Center for Computational Astrophysics, Flatiron Institute, 162 5th Ave, New York, NY 10010, USA*
[8]*INAF-Astronomical Observatory of Trieste, I–34143 Trieste, Italy*
[9]*University of Birmingham School of Physics and Astronomy, Edgbaston, Birmingham, England*

Accepted 2018 February 17. Received 2018 February 12; in original form 2017 November 6

ABSTRACT

It is well known that galaxies falling into clusters can experience gas stripping due to ram pressure by the intra-cluster medium. The most spectacular examples are galaxies with extended tails of optically bright stripped material known as 'jellyfish'. We use the first large homogeneous compilation of jellyfish galaxies in clusters from the WINGS and OmegaWINGS surveys, and follow-up MUSE observations from the GASP MUSE programme to investigate the orbital histories of jellyfish galaxies in clusters and reconstruct their stripping history through position versus velocity phase-space diagrams. We construct analytic models to define the regions in phase-space where ram-pressure stripping is at play. We then study the distribution of cluster galaxies in phase-space and find that jellyfish galaxies have on average higher peculiar velocities (and higher cluster velocity dispersion) than the overall population of cluster galaxies at all cluster-centric radii, which is indicative of recent infall into the cluster and radial orbits. In particular, the jellyfish galaxies with the longest gas tails reside very near the cluster cores (in projection) and are moving at very high speeds, which coincides with the conditions of the most intense ram pressure. We conclude that many of the jellyfish galaxies seen in clusters likely formed via fast (∼1–2 Gyr), incremental, outside-in ram-pressure stripping during first infall into the cluster in highly radial orbits.

Key words: galaxies: clusters: intracluster medium – galaxies:evolution – galaxies: ISM – galaxies: peculiar.

1 INTRODUCTION

Numerous studies have shown that cosmic environment plays a key role in transforming galaxies and quenching their star formation (see Boselli & Gavazzi 2006, and references therein). The physical mechanisms responsible for such transformations can be divided into two main types:

(i) Gravitational or tidal mechanisms can affect both the stars and the gas within galaxies. They include galaxy–galaxy interactions and mergers (Barnes & Hernquist 1996), interactions between galaxies and the gravitational potential of the host cluster (Byrd & Valtonen 1990), and the so-called 'harassment', or cumulative high-speed encounters between galaxies (Moore et al. 1996)

(ii) Hydrodynamical interactions between cluster galaxies' gaseous component and the hot intra-cluster medium (ICM) can result in gas stripping due to ram pressure (Gunn & Gott 1972), thermal evaporation (Cowie & Songaila 1977), or turbulent/viscous stripping (Nulsen 1982).

There is mounting evidence that ram-pressure stripping is one of the most effective mechanisms quenching galaxies in clusters. Simulations show that ram-pressure stripping can effectively

★ E-mail: yara.jaffe@uv.cl

© 2018 The Author(s)
Published by Oxford University Press on behalf of the Royal Astronomical Society

Downloaded from https://academic.oup.com/mnras/article/476/4/4753/4904145 by CIS Psicologia Biblioteca F.Metelli - Universita degli Studi di Padova user on 14 October 2020

remove cold gas from galaxies, and in some cases temporarily enhance the star-formation activity before quenching it completely (see e.g. Steinhauser, Schindler & Springel 2016, and references therein). The most striking evidence supporting ram-pressure stripping comes from observations of neutral gas (H I) in nearby galaxies located inside clusters (Haynes, Giovanelli & Chincarini 1984; Cayatte et al. 1990; Vollmer et al. 2001; Kenney, van Gorkom & Vollmer 2004; Chung et al. 2009; Jaffé et al. 2015; Yoon et al. 2017) or even groups (Verdes-Montenegro et al. 2001; Rasmussen, Ponman & Mulchaey 2006; Rasmussen et al. 2008; Jaffé et al. 2012; Hess & Wilcots 2013). Such observations show how cold gas can indeed be removed from infalling cluster galaxies.

In some cases, stars are formed in the stripped gas (Kenney & Koopmann 1999; Yoshida et al. 2008; Kenney et al. 2014), and can thus be identified from ultraviolet (UV) or optical images. The most striking examples of stripped galaxies with new stars tracing the stripped tails are the so-called 'jellyfish' galaxies. Estimates based on small blind Hα surveys of Coma and A1367 indicate that the fraction of cluster late-type galaxies with these features is close to 40 per cent (Boselli & Gavazzi 2014).

Numerous studies have focused on individual jellyfish galaxies (Merluzzi et al. 2013; Ebeling, Stephenson & Edge 2014; Fumagalli et al. 2014; Rawle et al. 2014; Fossati et al. 2016), and more recently, the first systematic searches for such objects at low and intermediate redshift have been conducted (McPartland et al. 2016; Poggianti et al. 2016). In particular, a dedicated ongoing integral-field spectroscopy survey with MUSE on the VLT has started to reveal with great detail the physics of gas removal processes in galaxies across a wide range of mass and environment (GASP; Poggianti et al. 2017b). The first results of GASP confirmed the stripped nature of the jellyfish candidates observed so far, showing spectacular evidence for ram-pressure stripping in action (Bellhouse et al. 2017; Fritz et al. 2017; Gullieuszik et al. 2017; Poggianti et al. 2017b, 2017a).

In addition to detailed observations and simulations of individual galaxies in clusters, a useful approach to study galaxy evolution in dense environments is to understand the assembly history of clusters. Pioneering work studying the position and velocities of different galaxy populations in clusters established the infall of spirals into clusters (Colless & Dunn 1996; Mohr, Geller & Wegner 1996; Biviano et al. 1997). A particularly useful tool to visualize the migration of galaxies from the field into clusters is thus position versus velocity phase-space diagrams, as they reflect the virialization state of a cluster, and contain information about the orbital history of cluster galaxies. In the last decades, several works have studied the location of different populations of cluster galaxies in projected phase-space to infer their time since infall (Vollmer et al. 2001; Mahajan, Mamon & Raychaudhury 2011; Oman, Hudson & Behroozi 2013; Hernández-Fernández et al. 2014; Haines et al. 2015; Muzzin et al. 2014; Jaffé et al. 2015, 2016; Oman & Hudson 2016; Yoon et al. 2017; Rhee et al. 2017).

Despite known projection effects (see discussion in Oman et al. 2013; Rhee et al. 2017), phase-space diagrams can further be used to identify different cluster mechanisms that affect galaxies during their passage, such as ram-pressure stripping of gas (Vollmer et al. 2001; Jaffé et al. 2015; Yoon et al. 2017) and tidal mass loss (Rhee et al. 2017). In particular Jaffé et al. (2015) compared the position of observed cluster galaxies with H I data with mock data to reconstruct the effect of ram-pressure stripping as a function of time since infall into the cluster. They show that significant gas stripping occurs on first infall and that galaxies gradually become H I-poor. In a follow-up study, Jaffé et al. (2016) further demonstrated that the gas removal from galaxies can be accompanied by an initial enhancement of the star-formation activity, followed by a slow quenching (see also Haines et al. 2015).

In this paper we investigate the orbital histories of jellyfish galaxies in low redshift clusters and the effect of ram-pressure stripping by the ICM. To achieve this, we compare the projected position and velocity of a large sample of cluster jellyfish candidates from Poggianti et al. (2016, P16 from now onwards) and a sub-sample of confirmed jellyfish galaxies from the GASP survey, with the control parent sample of cluster galaxies from WINGS (WIde-field Nearby Galaxy-cluster Survey; Fasano et al. 2006; Moretti et al. 2014) and its extension Omega WINGS (Gullieuszik et al. 2015; Moretti et al. 2018). In Section 2 we summarize the data available, and describe the sample of clusters, cluster galaxies, jellyfish candidates and confirmed jellyfish. We also separate the jellyfish galaxies observed with MUSE into four different categories related to their stripping stages. In Section 3 we construct analytic models of ram-pressure stripping for two (low and high-mass) clusters and two (low- and high-mass) galaxies, and identify the regions in position versus velocity phase-space diagrams where ram-pressure stripping is effective at removing gas from the galaxies in the different cases. In Section 4 we use the constructed models to interpret the spatial and velocity distribution of jellyfish galaxies in relation to their stripping stage. Moreover, we compare the velocity distributions of different galaxy populations to study their virialization states and their orbital types. In Section 5 we summarize our findings and draw conclusions.

Throughout this paper we assume a concordance ΛCDM cosmology with $\Omega_M = 0.3$, $\Omega_\Lambda = 0.7$, and $H_0 = 70\,km\,s^{-1}\,Mpc^{-1}$. We adopt a (Chabrier 2003) initial mass function in the mass range $0.1–100 M_\odot$.

2 DATA SET

2.1 The galaxy clusters

This paper makes use of the sample of cluster galaxies from WINGS (Fasano et al. 2006; Moretti et al. 2014) and its extension Omega WINGS (Gullieuszik et al. 2015; Moretti et al. 2018).

WINGS is a multiwavelength survey of 76 galaxy clusters at $0.04 < z < 0.07$, selected in X-rays from the ROSAT All Sky Survey (Ebeling et al. 1996, 1998, 2000). The core of the survey are B and V imagings (Varela et al. 2009) that cover the central 34arcmin × 34 arcmin of the clusters, reaching out to at least $0.6\times R_{200}$.[1] Complementary spectroscopic observations were obtained for a sub-sample of 48 clusters with WYFFOS@WHT and 2dF@AAT (Cava et al. 2009).

OmegaWINGS is an extension of WINGS that quadruples the area covered for a sub-sample of the clusters, allowing the study of the effect of cluster environment on galaxies well beyond the virial radius. Imaging in the *u*, *B*, and *V* bands were obtained with OmegaCAM@VST for 46 of the WINGS clusters over an area of $\sim$1 deg^2 (Gullieuszik et al. 2015). The spectroscopic follow-up has been obtained for a sub-sample of 33 clusters with the 2dFdr@AAT (Moretti et al. 2018).

The clusters span a wide range of velocity dispersion (σ_{cl} ~500–1300 km s^{-1}; Cava et al. 2009; Moretti et al. 2018) and X-ray

[1] R_{200} is defined to be the radius delimiting a sphere with interior mean density 200 times the critical density. It is typically used as an approximation for the cluster virial radius

Downloaded from https://academic.oup.com/mnras/article/476/4/4753/4904145 by CIS Psicologia Biblioteca F.Metelli - Universita degli Studi di Padova user on 14 October 2020

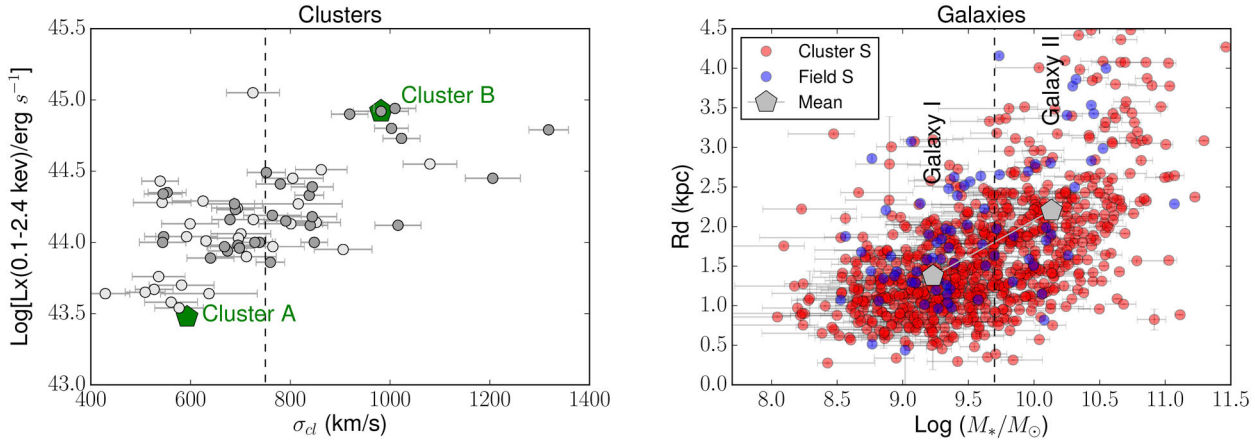

Figure 1. Left: cluster velocity dispersion ($\sigma_{\rm cl}$, with error bars) versus the X-ray luminosity (L_X) of the WINGS/OmegaWINGS clusters used in this work (all grey points). Clusters with spectroscopic completeness $>$ 50 per cent are highlighted with darker grey symbols. Right: The stellar mass ($M\star$) versus disc scale length (R_d) of all the cluster and field spirals (S) from the WINGS/OmegaWINGS samples with a redshift. Error bars for both quantities are plotted, but note that for R_d the errors are almost always smaller than the symbol. The green pentagons indicate the properties of the model clusters A and B (left) and model galaxies I and II (right) discussed in Section 3.1 (see also Tables 1 and 2).

luminosity ($L_X \sim (0.2 - 5) \times 10^{44}$ erg s^{-1} Ebeling et al. 1996, 1998, 2000), as shown in the left-hand panel of Fig. 1. Since the clusters also span a range of redshifts ($0.04 < z < 0.07$), and thus sizes in the sky, the radial coverage and completeness of the spectroscopy can vary significantly. However, the sample of all WINGS/OmegaWINGS clusters covers at least $\sim$1 $\times$ R_{200} and up to $\sim$3.5 $\times$ R_{200}. 32 out of the 76 clusters have a global spectroscopic completeness (calculated both as a function of V-band magnitude and radial projected distance from the BCG) higher than $\approx$ 50 per cent (see table 1 in Paccagnella et al. 2017). In this paper we use the full sample of WINGS/OmegaWINGS clusters (unless otherwise specified) noting that at cluster-centric distances $>R_{200}$ biases originated by spectroscopic incompleteness could be present.

2.2 The galaxy population

In the fields of the WINGS/OmegaWINGS clusters there are 42 816 galaxies with a spectroscopic redshift. 17 957 of them are classified as cluster members, based on the 3σ clipping method.

Morphologies of the WINGS galaxies were obtained applying the MORPHOT classification tool to the images, which closely reproduces the visual classification of ellipticals, lenticulars and spirals (Fasano et al. 2012; Moretti et al. 2014). Effective radii ($r_{\rm eff}$) from single-Sérsic fits were obtained using the GASPHOT tool (Pignatelli, Fasano & Cassata 2006; D'Onofrio et al. 2014). Since this paper focuses on infalling disc galaxies (modelled in Section 3.2), we compute the disc scale-length (r_d) for the disc galaxies (Sérsic index $n \sim 1$) with spiral morphologies (T-type $>$0 from MORPHOT) assuming $r_d = r_{\rm eff}/1.6783$, which is true for $n = 1$.

Other galaxy properties were derived fitting the fibre spectra with the spectro-photometric model SINOPSIS (SImulatiNg OPtical Spectra wIth Stellar population models; Fritz et al. 2007, 2011, 2014). The model utilizes the stellar population synthesis technique to reproduce the observed spectra. The output of the model includes star formation rates (SFRs) and stellar masses (M_*), among other quantities. In this paper we use stellar masses locked into stars that are in the nuclear-burning phase plus stellar remnants. The stellar masses of the cluster galaxies ranges between 10^8 and $10^{12} M_\odot$ (mean 6.3 $\times$ $10^9 M_\odot$). The right-hand panel of Fig. 1 shows the galaxy mass as a function of size for the spiral galaxy population in and outside the clusters. The correlation between galaxy mass and size has a scatter between $\sim$0.5 and 0.9 kpc in the stellar mass range from 10^9 to 10^{11} M$_\odot$.

2.3 The sub-sample of jellyfish candidates

The focus of this paper is to study the environmental history of jellyfish or heavily stripped galaxies in clusters. We use the jellyfish candidate catalogue of P16 that contains 409 nearby galaxies with optical signatures suggestive of gas stripping in a wide range of environments from the samples of WINGS, OmegaWINGS, and PM2CG (Calvi, Poggianti & Vulcani 2011), a field comparison sample, not considered in this paper. The jellyfish galaxy candidates were split into distinct 'classes' (JClass) from visual inspection of B-band images:

(i) JClass 5 and 4 correspond to the most convincing cases of stripping. They include the classical jellyfish galaxies with clear tentacles of stripped material.
(ii) JClass 3 are probable cases of stripping with clear one-sided asymmetries.
(iii) JClass 2 and 1 are the weakest cases of stripping.

P16 showed that the main bodies of the jellyfish candidates are mostly discy, with stellar masses ranging from 10^9 to $10^{11.5}$M$_\odot$. The same authors showed that, although the jellyfish galaxies span a similarly broad range of stellar masses and host cluster mass as the parent sample of WINGS/OmegaWINGS galaxies, they exhibit enhanced star-formation rates (by a factor of $\gtrsim$2) compared to non-stripped galaxies of similar stellar mass. Of the jellyfish candidates with a spectroscopic redshift, 70 per cent are cluster members. However, P16 found that the incidence of jellyfish with a spectroscopic redshift from WINGS/OmegaWINGS did not show a clear correlation with cluster velocity dispersion or X-ray luminosity.

2.4 Confirmed jellyfish galaxies

The ongoing GASP survey will observe over 100 jellyfish candidates from P16 as well as a control sample of non-stripped galaxies. So far, 80 of the GASP galaxies have been observed with MUSE.

Downloaded from https://academic.oup.com/mnras/article/476/4/4753/4904145 by CIS Psicologia Biblioteca F.Metelli - Universita degli Studi di Padova user on 14 October 2020

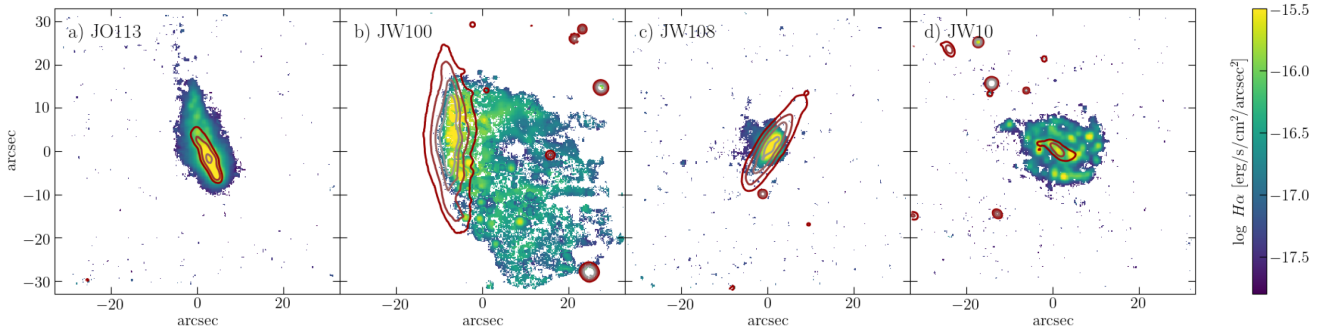

Figure 2. H α flux emission maps (colourbar) on top of isophotes of H α continuum in steps of 0.5 mag arcsec^{-2} (red contours) for 4-example GASP galaxies in different stripping stages. From left to right: (a) A galaxy with moderate signs of 'Stripping'; (b) a galaxy featuring very long gas tails indicative of 'Extreme-stripping'; (c) a truncated 'Post-stripping' galaxy; and (d) a disturbed galaxy where the physical cause of the disturbance is unclear ('?').

Here we focus on the sub-sample of 49 of the GASP jellyfish in clusters observed to date.

From the MUSE data cubes, we have created maps of the stellar (continuum) and gas (H α) components of the galaxies (see examples in Fig 2 and in Bellhouse et al. 2017; Fritz et al. 2017; Gullieuszik et al. 2017; Poggianti et al. 2017b, 2017a). These maps were used to visually re-classify the galaxies according to their apparent stripping stage into the following categories:

(i) 'Extreme-stripping': long one-sided gas tails comparable or larger than the stellar diameter.
(ii) 'Post-stripping': truncated gas discs that are smaller than the stellar disc.
(iii) 'Stripping': any other clear sign of stripping, such as the presence of a disturbed gaseous component relative to the stars.
(iv) '?': complex disturbed morphology that does not allow us to conclude that ram-pressure stripping is the (only) mechanism at play. A couple of these objects show galaxies nearby that could potentially be interacting with them.

We emphasize that the component that is disturbed in the jellyfish galaxies is the gas. The stars are undisturbed and rotate smoothly within the disc (not shown here, but see Bellhouse et al. 2017; Fritz et al. 2017; Gullieuszik et al. 2017; Poggianti et al. 2017b), which supports the idea that its ram-pressure stripping rather than tidal effects giving rise to the jellyfish morphology. Out of the 49 cluster galaxies observed by GASP, we found that 22 are experiencing moderate gas stripping ('Stripping'), 12 'Extreme-stripping' and 4 'Post stripping'. The remaining 16 show complex morphologies ('?'). Fig. 2 shows composite images from MUSE data of a few examples jellyfish galaxies observed by GASP in the different categories. The effect of the ram-pressure 'wind' is visible from the H α morphologies of the stripped galaxies in panels a, b, and c. Moreover, the fact that jellyfish galaxies still hold gas in their cores is indicative of outside-in stripping. This hypothesis is also supported by the gas kinematics and metallicity gradients seen in jellyfish galaxies (Bellhouse et al. 2017; Fritz et al. 2017; Gullieuszik et al. 2017; Poggianti et al. 2017b).

From the classification exercise it became clear that the distribution of H α gas with respect to the stellar component (this paper) is a much more representative and quantitative way to determine the stripping stage of a galaxy than through broad-band (BB) imaging (P16), which only shows the tip of the iceberg of the stripped gas. Nevertheless, the classification of GASP galaxies is mostly in agreement with the JClass classification of P16: GASP galaxies visibly undergoing 'Extreme stripping' also have the highest JClass numbers, while the 'stripped' and 'post-stripped' galaxies have JClass$\sim$3. However, weak jellyfish features in BB optical images are not able to distinguish between stripping and post-stripping.

In this work we treat the confirmed jellyfish galaxy sample (i.e. galaxies observed by GASP so far that show signs of stripping) separately from the bigger sample of jellyfish candidates from Poggianti et al. (2016), and utilize MUSE data when available to compute spectroscopic redshifts (and thus cluster membership), and stellar masses. The redshift was obtained from the spectra in the central part of the galaxy, while the masses were computed from SINOPSIS, using the integrated spectra within the lowest surface brightness stellar isophote defined from the continuum underlying H α, down to $\sim 1 \times \sigma$ from the background level (see section 6.5 in Poggianti et al. 2017b, for details).

Finally, it is important to note that the detectability of stripped gas tails (and thus jellyfish galaxies) is expected to be sensitive to the lifetime of the tail before it is mixed (which is very poorly understood), as well as the inclination of the galaxy motion with respect to the observer. Between galaxies being stripped along the line of sight and galaxies moving along the plane of the sky, the latter are more likely to display extended visible tails that could facilitate their identification as 'jellyfish'. However, we note that we have confirmed cases of line-of-sight stripping in our sample. The most extreme of such examples is the GASP galaxy JO201, presented in Bellhouse et al. (2017), which not only has clear tails of stripped gas along the plane of the sky (due to a small inclination angle with respect to the observer), but also a complex gas kinematics that impressively shows the stripped material that is dragging behind the galaxy. However, most of the other galaxies undergoing 'Extreme stripping' (e.g. JO204: Gullieuszik et al. 2017), are more likely to be travelling mostly in a direction perpendicular to the observer.

3 MODELLING RAM-PRESSURE STRIPPING ANALYTICALLY

In the following we present models of ram-pressure stripping intensity based on two different cluster models and two different galaxy models.

Ram pressure by the ICM was defined by Gunn & Gott (1972) as:

$$P_{\rm ram} = \rho_{\rm ICM}\, \Delta v^2_{\rm cl(3D)}, \quad (1)$$

where $\Delta v_{\rm cl(3D)}$ is the differential 3D velocity of the galaxy with respect to the cluster centre, and $\rho_{\rm ICM}$ the density of the ICM, which decreases with cluster-centric radius.

Downloaded from https://academic.oup.com/mnras/article/476/4/4753/4904145 by CIS Psicologia Biblioteca F.Metelli - Universita degli Studi di Padova user on 14 October 2020

Table 1. Properties of the model clusters: low-mass cluster (A) and high-mass cluster (B). The columns are: cluster, velocity dispersion, R_{200}, β parameter from equation (2), central gas density ρ_0. References for Cluster A: Mei et al. (2007); McLaughlin (1999); Ferrarese et al. (2012). Reference for Cluster B: Chen et al. (2007).

Model name	$\sigma_{\rm cl}$ (km s^{-1})	R_{200} (Mpc)	β	ρ_0 (10^{-23}Kg m^{-3})	R_c (kpc)
Cluster A	593	1.55	0.5	6.69	13
Cluster B	982	2.37	0.5	4.30	82

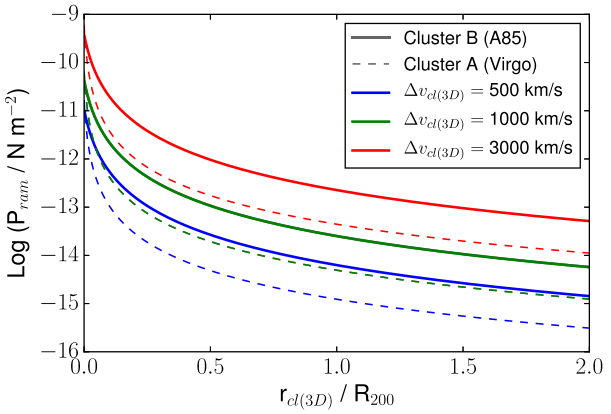

Figure 3. The ram-pressure intensity profile for the model clusters A (solid lines) and B (dashed lines) for different differential velocities of an infalling galaxy.

When $P_{\rm ram}$ exceeds the anchoring self-gravity provided by the galaxy ($\Pi_{\rm gal}$), the galaxies' gas is stripped.

In the following, we create general cluster (Section 3.1) and galaxy (Section 3.2) models that can conveniently be used in other studies to predict the amount of gas stripped (Section 3.3) and define ram-pressure stripping zones in position versus velocity phase-space diagrams (Section 3.4).

3.1 Cluster models

The ICM gas density profile of clusters is typically parametrized with a β model (Cavaliere & Fusco-Femiano 1976), as

$$\rho_{\rm ICM}(r_{\rm cl(3D)}) = \rho_0 \left[1 + \left(\frac{r_{\rm cl(3D)}}{R_c}\right)^2\right]^{-3\beta/2}, \quad (2)$$

where ρ_0 is the gas density at the cluster centre, $R_{\rm c}$ the core radius, and $r_{\rm cl(3D)}$ the 3D distance from the cluster centre.

We use two cluster models that seek to cover the extremes of the cluster population. Their properties are listed in Table 1. Cluster A represents low-mass cluster population. Hence, we use the ICM of the Virgo cluster as reference as it is well studied in the context of ram-pressure stripping (e.g. Vollmer et al. 2001; Chung et al. 2009; Boselli et al. 2011; Ferrarese et al. 2012; Yoon et al. 2017), and widely referenced in galaxy evolution studies. Cluster B instead represents high mass clusters. In this case we used Abell 85 (A85) as reference as it is one of the most massive clusters in WINGS and it is also well studied (e.g. Kempner, Sarazin & Ricker 2002; Durret, Lima Neto & Forman 2005; Bravo-Alfaro et al. 2009; Aguerri et al. 2017).

Fig. 3 shows $P_{\rm ram}$ as a function of distance from the core of Virgo (Cluster A, dashed line) and A85 (Cluster B, solid line), computed using equations (1) and (2) for different galaxy velocities.

Table 2. Properties of the model galaxies: low-mass galaxy (I), and high-mass galaxy (II). Columns are: stellar masses ($M\star$), gas fractions (include *HI* and H_2, from Popping, Somerville & Trager 2014), disc scale-length (r_d, mean values of the OmegaWINGS galaxies in the low- and high-mass bins shown in the right-hand panel of Fig. 1), and the resulting anchoring force of the galaxy ($\Pi_{\rm gal}$, computed from equation 3).

Model name	$\log M\star$ ($M_\odot$)	$M_{\rm gas}/M\star$	R_d (kpc)	$\Pi_{\rm gal(r=0)}$ (Nm^{-2})
Galaxy I	9.2	0.7	1.4	9.2×10^{-12}
Galaxy II	10.1	0.3	2.2	8.9×10^{-11}

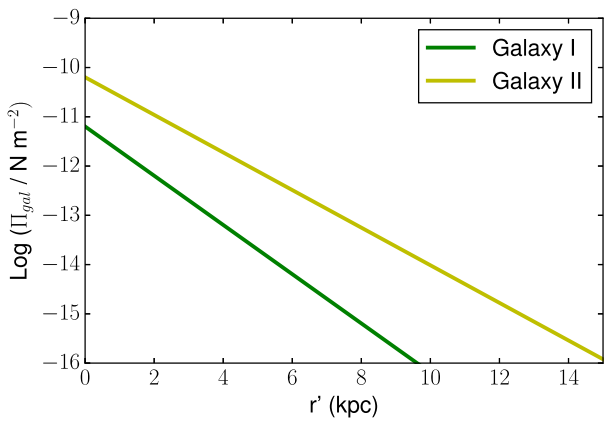

Figure 4. The anchoring force as a function of radial distance from the galaxy centre for two model galaxies (I and II, as indicated).

Note that, although at the cluster centres $P_{\rm ram}$ is similar in both clusters, at increasing $r_{\rm cl(3D)}$ they quickly start to differ by almost an order of magnitude, and if we consider the typical velocities of galaxies in each cluster ($\sigma_{\rm cl}$ from ∼400 to ∼1300 km s^{-1}), the difference can become even larger.

3.2 Galaxy models

To assess whether the cluster can strip the gas in an infalling galaxy, it is necessary to have an estimate of the orbit and also the galaxy's anchoring (restoring) force or self-gravity.

The galaxies's anchoring force, $\Pi_{\rm gal}$, can be modelled assuming the form:

$$\Pi_{\rm gal}(r') = 2\pi G \Sigma_{\rm s} \Sigma_{\rm g}, \quad (3)$$

where $\Sigma_{\rm s}$ and $\Sigma_{\rm g}$ are the density profiles of the stellar and gaseous discs, respectively.

Given that most jellyfish galaxies are gas-rich late-type galaxies (although see the peculiar cases of stripping presented in Sheen et al. 2017, and Moretti et al. submitted), we assume an exponential (disc) profile for the density of both the gas and the stars:

$$\Sigma(r') = \Sigma_0 e^{-r'/R_d}, \quad (4)$$

where r' is the radial distance from the centre of the galaxy, R_d is the disc scale length, $\Sigma_0 = M_d/(2\pi R_d^2)$, and M_d is the mass in the disc.

In order to create generic disc galaxy models, we explored the properties of the discy spiral galaxies in WINGS/OmegaWINGS, plotted in the right-hand side of Fig. 1. We distinguished field (blue) from cluster (red) galaxies and found no strong segregation in either mass or size. Since the galaxies are disc-dominated, we assume that the stellar disc ($M_{d,\star}$) is equivalent to the total stellar mass of the

Downloaded from https://academic.oup.com/mnras/article/476/4/4753/4904145 by CIS Psicologia Biblioteca F.Metelli - Universita degli Studi di Padova user on 14 October 2020

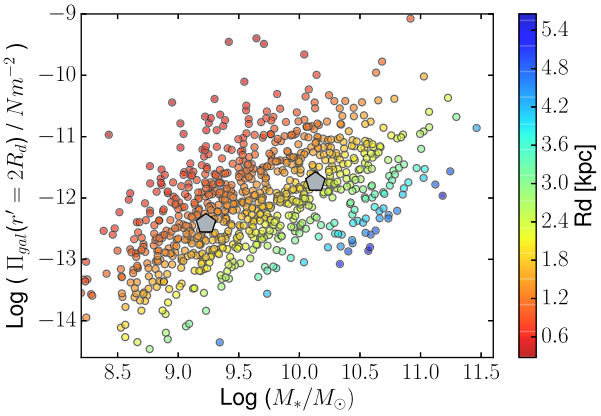

Figure 5. The anchoring force at $r' = 2 \times R_d$ as a function of stellar mass for all spiral galaxies in our (cluster plus field) sample. The grey pentagons correspond to the model galaxies I and II.

galaxy. We discuss the impact of the inclusion of a bulge component in Section 3.5.

Another parameter we had to assume was the gas fraction. We used as reference the work of Popping et al. (2014), who show the variation of H I and H_2 content of disc-dominated galaxies (B/T<0.4) as a function of stellar mass. In the mass range $10^8 < M_\star < 10^{11.5} M_\odot$ the fraction of H I mass relative to stellar mass varies between 150 and 5 per cent. For $10^{10} M_\odot$ galaxies the H I gas fraction is ∼20 per cent. To this fraction we need to add the H_2 gas component, which is less abundant and varies much less with $M_\star$ (from 10 to 4 per cent in the above-mentioned mass range).

We assume that the extent of the gas ($r_{d,g}$) is larger than the size of the stellar disc ($r_{d,\star}$) by a factor of 1.7. This value corresponds to the H I to optical radius of non-H I-deficient spiral galaxies in Virgo (Cayatte et al. 1994)

Having a good characterization of the galaxies, we can now compute Π_{gal}. We do this for two idealized galaxies (Galaxies I and II) that represent the mean of the low ($<5 \times 10^9$ M$_\odot$) and high ($>5 \times 10^9 M_\odot$) mass galaxies in our galaxy sample (see the right-hand panel of Fig. 1). The properties of the model galaxies are listed in Table 2, and the resulting Π_{gal} profile as a function of r is shown in Fig. 4.

For completeness and future reference, Fig. 5 further shows Π_{gal} computed at $r = 2 \times R_d$ as a function of stellar mass for WINGS/OmegaWINGS galaxies, colour-coded by disc scale length. The figure highlights the interconnected role of stellar mass and size in the estimation of the restoring force of a galaxy. It is interesting to notice that a dwarf galaxy with $M_\star = 1 \times 10^9 M_\odot$ can in principle have the same central restoring force as a galaxy 100 times more massive ($M_\star = 1 \times 10^{11}M_\odot$) if the sizes are very different. Galaxies with higher central densities (red symbols) have stronger anchoring pressure.

3.3 Computing the amount of stripped gas

Having a model of the galaxy (Section 3.2) and the cluster (Section 3.1) that it is infalling into, it is possible to estimate the amount of stripping (total gas mass lost by the galaxy) by directly comparing P_{ram} (Fig. 3) with Π_{gal} (Fig. 4). We summarize the steps below:

(i) Obtain the position and velocity of the galaxy (or galaxies) within its host cluster. These are the phase-space coordinates. Note that because these quantities come from photometric and spectroscopic observations of the cluster, one can only measure projected distances (r_{cl}) and line-of-sight velocities (Δv_{cl}), which are lower limits to the real (3D) values (see discussion in Section 3.5).

(ii) Using the position and velocity obtained in (i), compute P_{ram} from equations (1) and (2) if ρ_{ICM} is known (from X-ray observations of the cluster of interest). Alternatively, a scaled estimate can be inferred from the relations displayed in Fig. 3.

(iii) Compute the anchoring force of the galaxy, Π_{gal} from equations (3) if the galaxy mass, size, and morphological type are known, or get a scaled estimate from the relations plotted in Figs 4 and 5.

(iv) Compare P_{ram} obtained in (ii) with the radial profile of Π_{gal} for the galaxy obtained in (iii), and identify the radius r_t within the galaxy disc at which $P_{ram} = \Pi_{gal}$. Because ram-pressure strips the disc gas outside-in, r_t corresponds to the radius of stripping, or 'truncation' radius.

(v) From r_t we can further compute the remaining gas mass in the galaxy following:

$$f = 1 + \left[e^{-r_t/R_d} \left(\frac{-r_t}{R_d} - 1 \right) \right], \quad (5)$$

This equation is directly derived from the mass distribution of an exponential disc assuming the remaining gas is enclosed inside the truncation radius ($r' < r_t$).

3.4 Ram-pressure stripping in phase-space

Position versus velocity phase-space diagrams are very useful tools to study the orbital histories of galaxies in clusters. Moreover, these diagrams can be utilized to study cluster processes such as ram-pressure stripping (Hernández-Fernández et al. 2014; Jaffé et al. 2015; Yoon et al. 2017) or tidal mass loss (Rhee et al. 2017).

Fig. 6 shows schematically the position versus velocity phase-space location of simulated cluster galaxies from Rhee et al. (2017), separated by time since infall and normalized by cluster size and velocity dispersion. Infalling galaxies will approach the cluster centre gaining velocity, so they are located within the blue contours of the figure. After the galaxy has passed pericentre, it will inevitably 'bounce' back in phase-space but with lower velocity due to the combined effect of violent relaxation, dynamical friction, and the growth of the cluster. For this reason, galaxies that have been in the cluster for over a cluster crossing time will tend to gather near the centre of the cluster at lower velocities (red 'virialized' region). Note that the 'virialized' and 'Recent infalls' regions, although fundamentally different, have some overlap at high velocities in the inner part of the cluster ($r_{cl(3D)} < R_{200}$).

From the modelling described in Sections 3.1, 3.2, and 3.3, it is possible to construct regions in phase-space where ram-pressure stripping is at play. This is shown in the green 'cone' of Fig. 6, that represents as an example, the region where a low-mass galaxy (model Galaxy I) would be incrementally stripped (losing from 10 to 90 per cent of its gas) by ram pressure as it falls into a massive cluster (Cluster B). The different green curves further show the increasing effect of ram pressure with decreasing cluster-centric distance and increasing velocities, in accordance with equation (1). As more gas gets stripped (indicated by the percentages of total gas mass lost in the legend), the truncation radius will inevitably become smaller. Note that the green lines do not reach zero velocity because ram-pressure intensity depends on velocity squared.

It is important to highlight that the stripping region in phase-space depends on cluster mass and galaxy mass/size, with lower-mass, less concentrated galaxies being more vulnerable to stripping than massive galaxies. Ram-pressure stripping 'cones' generated by

Downloaded from https://academic.oup.com/mnras/article/476/4/4753/4904145 by CIS Psicologia Biblioteca F.Metelli - Universita degli Studi di Padova user on 14 October 2020

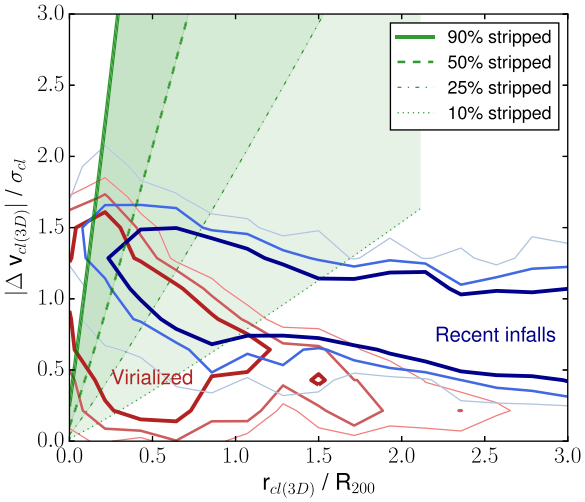

Figure 6. The position versus velocity phase-space diagram of 15 simulated group and cluster galaxies (mass range from 5×10^{13} to $1 \times 10^{15} M_{\odot}$) from Rhee et al. (2017, private communication), considering multiple lines of sight, separated into 'virialized' (entered the cluster >4 Gyr ago; red contours) and 'Recent infalls' (falling towards the cluster for the first time or recently entered the cluster <2 Gyr; blue contours). A galaxy is considered to enter the cluster when it has crossed R_{200} for the first time. The contours enclose 1000, 2500, and 5000 particles from lighter to darker colours, respectively. The axes have been normalized by cluster size (R_{200}) and cluster velocity dispersion (σ_{cl}) to allow the stacking of 15 simulated clusters with masses between 10^{13} and $10^{15} M_{\odot}$. The green area indicates the region where ram pressure by the ICM is able to strip 10 per cent (dotted line) to 90 per cent (solid lines) of the total gas mass of a low-mass galaxy (model galaxy I) falling in a massive cluster (model cluster B). For details, see Section 3, and Tables 1 and 2.

different clusters for different galaxies are shown in Fig. 8 and will be discussed in Section 4.

3.5 Caveats

There are several caveats to the simplistic ram-pressure stripping model presented in this section. We summarize the most important ones here:

(i) Scatter introduced by projection effects. Observationally, one measures projected radius in the plane of the sky and line-of-sight velocities. The 3D radius scales with the projected radius as $r_{\rm cl} = \cos(\varphi) r_{\rm cl(3D)}$, where φ is the projection angle, that can vary between 0 and $\pi/2$. On average, $r_{\rm cl} = \frac{2}{\pi} r_{\rm cl(3D)}$ but there is considerable scatter. The projected velocity is also a lower limit to the 3D velocity by a factor of $\sqrt{3}$ on average.
Despite the known projection effects, several works using cosmological simulations have shown that it is possible to separate the oldest from the most recently accreted cluster members in projected phase-space. Galaxies with intermediate time-since-infall (including backsplash galaxies) are harder to distinguish, as they overlap in phase-space with both the virialized and recent infall galaxies (Oman et al. 2013; Jaffé et al. 2015; Rhee et al. 2017). However, Yoon et al. (2017) recently showed that it is possible to identify the backsplash population combining the phase-space location of cluster galaxies with detailed H I observations, which they used as a proxy for the galaxy's stripping stage and thus time since infall.

(ii) The analysis presented in this section applies to disc galaxies. For non-disc galaxies the calculation of the restoring force should be altered.

(iii) The analysis also assumes the clusters are regular (dynamically relaxed), with a spherical β-profile for the ICM density (equation 2). For clusters with significant substructure, it should be noted that the intensity of ram pressure can be enhanced at places and inhomogeneous across the cluster and that the orbits (and thus velocities) of infalling galaxies can also be altered (Owers et al. 2012; Vijayaraghavan & Ricker 2013; Jaffé et al. 2016; McPartland et al. 2016). We note however that most of the clusters considered in this paper have a regular distribution of galaxies (both spatially and in velocity). Only a fraction ($\sim$1/3) of clusters show signs of galaxy substructure, but the contribution of such substructures are expected to become less significant when we stack all the clusters together in phase-space (cf. Section 4.1). Nevertheless, owing to the known importance of cluster and group mergers in the evolution of galaxies, we will use our sample of clusters to study the effect of cluster substructure and cluster mergers in the formation of jellyfish galaxies in a dedicated follow-up study.

(iv) The Gunn & Gott (1972) approximation assumes a face-on interaction between the galaxy and the ICM. Although simulations show that the inclination of the galaxy with respect to the cluster (i.e. the wind angle) can lead to complex behaviour (e.g. Abadi, Moore & Bower 1999; Vollmer et al. 2001), it has been shown that the amount of stripping is only significantly altered in the case of edge-on interactions (Roediger & Brüggen 2006), which are very rare.

(v) We assume that the disc galaxies are not stripped in any way before entering the cluster, which might not be the case if there were any pre-processing in lower density environments (see e.g. Jaffé et al. 2016).

(vi) Finally, we note that because our galaxy models assume a pure disc profile, they may have underestimated the true anchoring force by neglecting the contribution of the dark matter halo and bulge. In principle this could result in an overestimation of the gas stripping. We estimate the additional contribution of the bulge and dark matter halo using analytical models. Our test models consist of a Navarro, Frenk & White (1996, NFW) halo, a Hernquist (1990) profile for the bulge, and the same exponential discs of gas and stars of Galaxies I and II. We measure the restoring force for gas within $\sim 10 \times R_d$, near the plane of the galaxy, and we consider a wide range of halo concentrations (c = 10–30). We find that the contribution of the bulge and halo can be significant, but only in the very inner disc (at $<0.5 R_d$). At $2R_d$, the addition of both the bulge and halo increases the anchoring force by no more than a few percent, which we calculate has only a very mild impact on predicted truncation radii.

4 THE ORBITAL HISTORY OF JELLYFISH GALAXIES IN CLUSTERS

In the following, we use projected position and line-of-sight velocity information of the cluster jellyfish galaxies to infer the time since infall into the cluster, the eccentricity of the orbits, and the intensity of ram-pressure stripping exerted by the ICM, modelled in Section 3.

4.1 Jellyfish galaxies in phase-space

Fig. 7 shows the projected phase-space distribution of all the cluster members in our galaxy sample (orange background) stacked together in a 'master cluster'. The densest part of the plot (darker orange) corresponds to the 'virialized' part of the clusters. The location of jellyfish galaxies in phase-space is highlighted with

Downloaded from https://academic.oup.com/mnras/article/476/4/4753/4904145 by CIS Psicologia Biblioteca F.Metelli - Universita degli Studi di Padova user on 14 October 2020

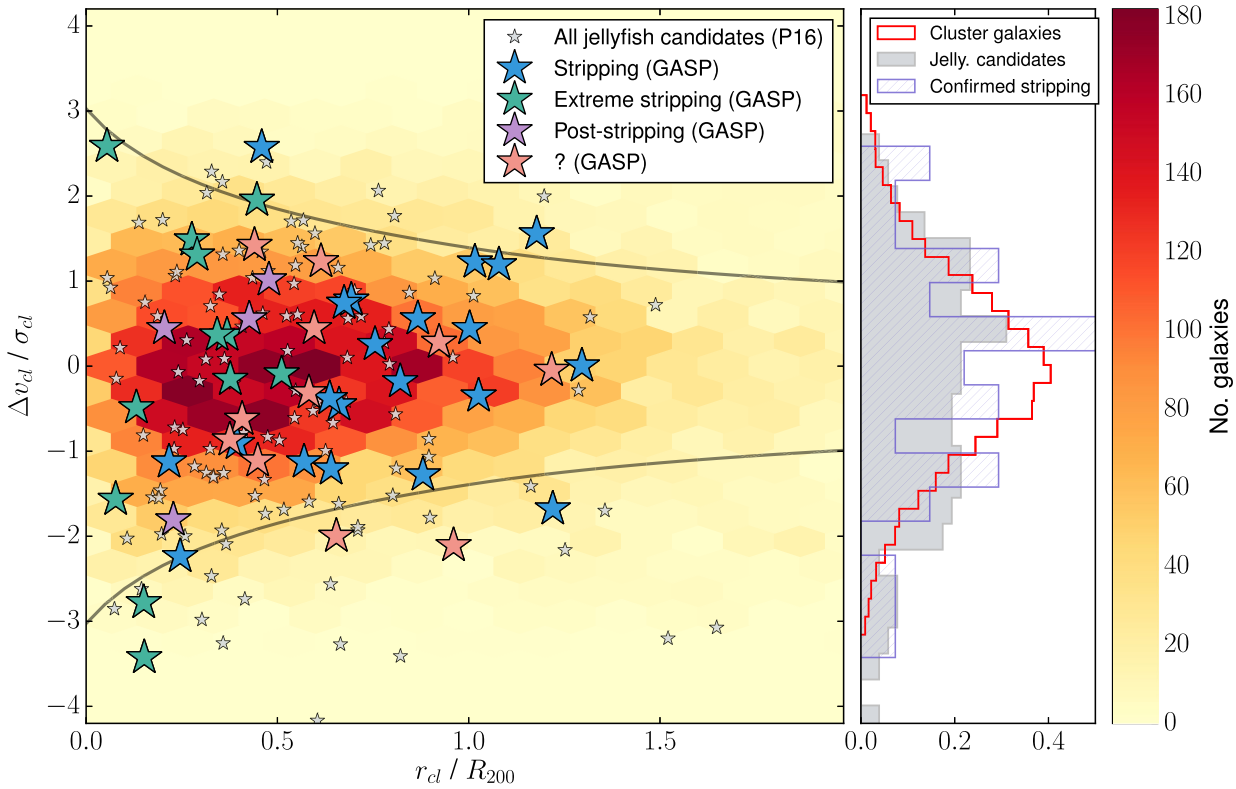

Figure 7. The location in projected position versus velocity phase-space of all the jellyfish galaxy candidates from P16 (small grey stars) and the ones observed with MUSE by GASP so far (larger colored stars), separated by stripping stage as indicated. The background shows the distribution of all WINGS/OmegaWINGS clusters with spectroscopic completeness >50 per cent stacked together (orange colorbar). The grey curve corresponds to the 3D (un-projected) escape velocity in a NFW halo with concentration $c = 6$ for reference. Note that, contrary to the absolute velocities plotted in the phase-space diagram of Fig. 6, the velocity axis in this plot has positive and negative values. To the right of the phase-space diagram, a plot shows the velocity distribution of the overall cluster population of galaxies (open red histogram), all the jellyfish candidates from P16 (filled grey histogram), and the galaxies observed by GASP that are confirmed stripping cases (i.e. 'Stripping', 'Extreme stripping', and 'Post-stripping; dashed blue histogram) at $r_{cl} < R_{100}$. All histograms have been normalized to unity for comparison.

stars on top of the overall cluster population. Smaller symbols correspond to jellyfish candidates from P16 while larger symbols represent confirmed jellyfish from GASP. Given the large size of the WINGS/OmegaWINGS cluster galaxy sample, we limited the cluster sample to the clusters with completeness >50 per cent to reduce biases, but plotted jellyfish galaxies in all clusters to increase the number count. We checked however that the distribution of jellyfish galaxies restricted to clusters with spectroscopic completeness >50 per cent in phase-space is very similar to the distribution of all jellyfish galaxies. In the region where there is higher spectroscopic coverage for all clusters ($r < R_{200}$) the incidence of jellyfish relative to the overall population of cluster galaxies peaks near the reference escape velocity curve, avoiding the virialized part of the cluster where most of the cluster members that are not currently undergoing stripping are. The difference in the distributions can be quantified with a 2D Kolmogorov–Smirnov (KS) test, which gives a very low probability (0.6 per cent) that the samples of stripping (P16 jellyfish; stars) and non-stripping (WINGS/OmegaWINGS; colourbar) cluster galaxies within $r_{cl} < R_{200}$ are extracted from the same parent distribution.

Focusing on the GASP galaxies, it is noticeable how the jellyfishes with longest tentacles of stripped material ('Extreme stripping'; green stars) are all located within $0.5 \times R_{200}$ and many are at $|\Delta v|/\sigma > 1$, which results in a broad velocity distribution. Their location coincides with the most favorable conditions for ram-pressure stripping within the cluster, which requires a small projected cluster-centric radius, and high absolute differential velocity with respect to the cluster redshift (see Section 3). In fact, in the first papers from the GASP series (Bellhouse et al. 2017; Fritz et al. 2017; Gullieuszik et al. 2017; Poggianti et al. 2017b) we have carefully compared the truncation radius measured from the H_α maps with the predictions from the position of three of these galaxies in phase-space. We found in all cases a good agreement between the predicted and measured stripping. In particular, we find that the galaxies have lost a significant fraction ($\gtrsim$ 15, 50, and 40 per cent) of their total gas mass during their first infall into the cluster. Moreover, hydrodynamical simulations of one of the galaxies (JO204; Gullieuszik et al. 2017) further confirm the estimated amount of stripping.

The galaxies with milder signatures of stripping ('Stripping'; blue stars in Fig. 7), unlike the 'extreme stripping' cases, are mostly located beyond $>0.5 \times R_{200}$, but they share the elevated velocities and wide velocity distribution with respect to the general cluster population (see histogram in the right-hand panel of Fig. 7). The distribution of both populations of stripped galaxies in phase-space coincides remarkably well with the region of 'recent infallers' defined from cosmological simulations in Rhee et al. (2017) and shown in Fig. 6. However, the distribution of galaxies undergoing

Downloaded from https://academic.oup.com/mnras/article/476/4/4753/4904145 by CIS Psicologia Biblioteca F.Metelli - Universita degli Studi di Padova user on 14 October 2020

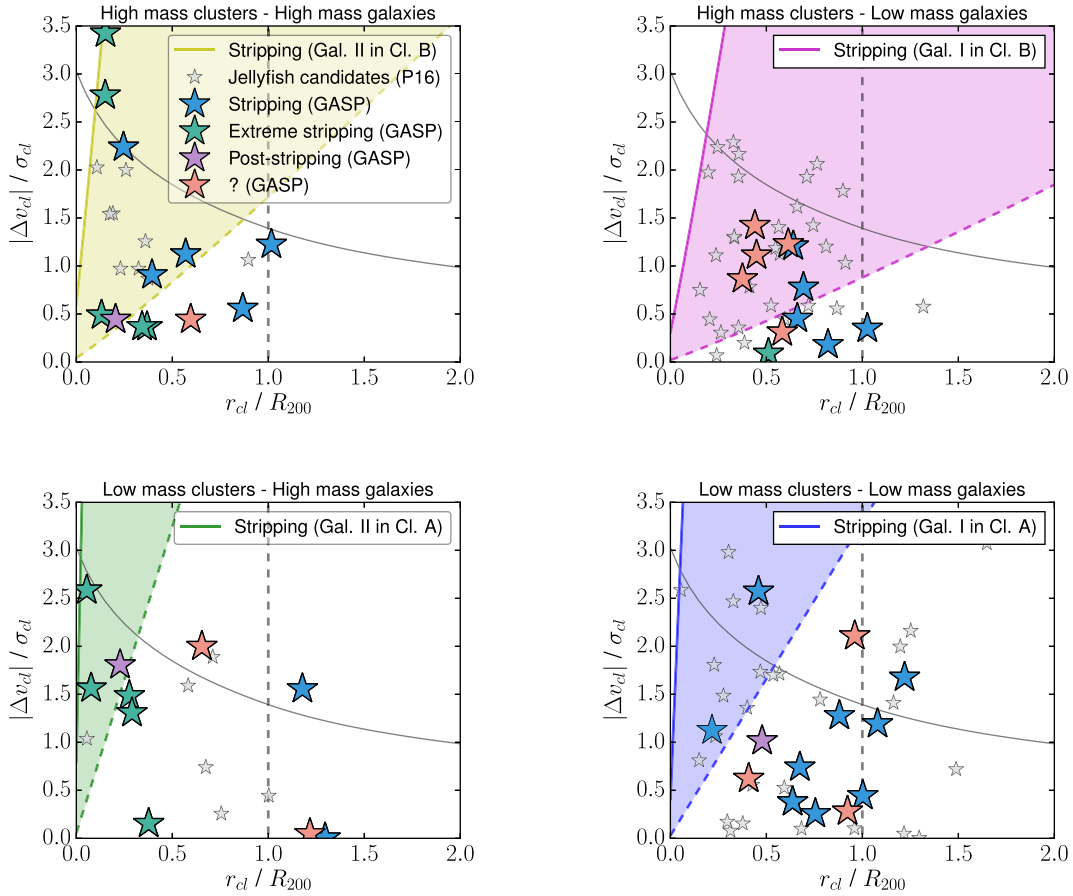

Figure 8. The location in position versus velocity phase-space of jellyfish galaxies in high mass clusters (top panels; $\sigma_{\rm cl} > 750\,{\rm km\,s^{-1}}$) and low mass clusters (bottom pa nels; $\sigma_{\rm cl} < 750\,{\rm km\,s^{-1}}$) separated in two bins of stellar mass: $>5 \times 10^9 M_\odot$ on the left-hand panels and $<5 \times 10^9 M_\odot$ on the right-hand panels. As in Fig. 7, grey stars correspond to the jellyfish sample of P16 while the bigger stars are the confirmed jellyfish galaxies from GASP. Lines of different intensities of ram pressure are indicated in each case: the dashed coloured lines indicate 10 per cent stripping of the total gas mass, while the solid line corresponds to 90 per cent stripping. The grey curve corresponds to the escape velocity in a NFW halo. The vertical dashed line indicates $r = R_{200}$, which is roughly the extent to which all clusters used have a high spectroscopic completeness.

moderate 'Stripping' is notably different from the 'Extreme stripping' galaxies. In fact, the KS probability that they are drawn from the same parent distribution is 0.026 per cent.

Interestingly, the galaxies with heavily truncated gas discs ('Post-stripping'; purple stars) are near the centre of the cluster, which indicates that they had an orbit which brought them close to the core of the cluster, where ram pressure is most intense. Although so far GASP has only observed 4 'post-stripping' galaxies, their moderate velocities could be interpreted as an indication of deceleration post-pericentric passage.

Finally, the galaxies with inconclusive gas morphologies ('?', orange stars) share common location with the moderately stripped galaxies, not ruling out the effect of ram pressure.

To assess the intensity of ram pressure that the galaxies could be experiencing, we split the sample of GASP galaxies in four bins, according to their stellar masses, and the masses of the clusters. We consider low mass galaxies all the galaxies with $M_\star < 5 \times 10^9 {\rm M}_\odot$ and high-mass galaxies $M_\star > 5 \times 10^9 {\rm M}_\odot$. Likewise, we separate cluster by mass, splitting them in velocity dispersion at $750\,{\rm km\,s^{-1}}$. Fig. 8 shows the phase-space distribution of jellyfish in those four bins. In each case, the area where ram-pressure stripping is at play (from 10 per cent to 90 per cent stripping) is indicated with a shaded colored area. The upper-right panel corresponds to the case of most efficient stripping, while the lower-left panel corresponds to the least efficient stripping, with gas loss only occurring in a limited range of distances and velocities. This is partly reflected in the larger number of jellyfish found in the top-right panel with respect to the lower-left, although there might be selection effects related to the impact of the viewing angle and stripping stage in the identification of jellyfish galaxies.

GASP galaxies undergoing 'Extreme stripping' (green stars in Fig. 8) are high mass galaxies in both low- and high-mass clusters. With only one exception, these galaxies are inside or near the zone where ram pressure is estimated to be most intense. It is important to keep in mind that the plotted velocities are lower limits to the real 3D velocities of the galaxies, and that these particular galaxies display long tails of stripped gas, which implies that a large component of their velocities are in the plane of the sky. In other words, it is likely that these galaxies would move up in the velocity direction in real 3D phase-space. Taking this into consideration, we conclude that galaxies classified as 'Extreme stripping' from their Hα morphologies are consistent with being subject to intense ram pressure close to pericentric passage (i.e. peak stripping). This result was partially shown in Fig. 4 of (Poggianti et al. 2017a), where among the 7 GASP galaxies with the strongest signatures of stripping observed with MUSE by then, the majority were found to host

Downloaded from https://academic.oup.com/mnras/article/476/4/4753/4904145 by CIS Psicologia Biblioteca F.Metelli - Universita degli Studi di Padova user on 14 October 2020

an AGN. All of these galaxies are located in the area of phase-space where ram-pressure stripping is the strongest, supporting the hypothesis that ram pressure can induce AGN activity. Ram-pressure stripping simulations by Tonnesen & Bryan (2012) show that the star-formation rate in the stripped tails depends on the amount of gas stripped and the ICM pressure. It is thus possible that only massive galaxies were able to keep their gas for long enough to still be gas-rich by the time they approach pericentre. If they pass close to the cluster core (as our 'Extreme stripping' galaxies do), the gas that is stripped will be able to form more stars. Another possibility is that massive galaxies will show bright (detectable) optical tails for longer than low-mass ones. We will investigate these possibilities with the full GASP sample in future studies.

It is interesting to note that many of the jellyfish galaxies with less extreme signs of stripping ('Stripping', blue stars in Fig. 8) are low-mass galaxies in low-mass clusters located outside the high-intensity stripping zone. As explained in Section 3.5, the main caveat in the interpretation of the distribution of galaxies in phase-space is the effect of projection, which makes the measured distances and velocities lower limits to the real values. The one-sided tails of jellyfish galaxies indicate that they are moving at least partially along the plane of the sky, which in turn means that their projected velocities are likely lower than their true value. It is not trivial to infer the 3D velocity of observed cluster galaxies but it is reasonable to argue that, on average, the measured (line-of-sight) velocities of jellyfish galaxies are more likely to be an underestimation of the real (3D) value in comparison to other cluster galaxies. Considering this, it is possible that, after removing projection offsets, many of these 'Stripping' jellyfish outside the high-intensity stripping zone in projected phase-space would be inside this zone if de-projected. Alternatively, it is possible that some of the jellyfish galaxies could reside in clusters with significant sub-structure (e.g. the Shapley supercluster), where multiple cluster centres are present and/or ram pressure is likely enhanced outside the cluster core. Although in our sample most clusters are not undergoing mergers, if we exclude the most unrelaxed clusters from the analysis, we find that the remaining jellyfish galaxies in phase-space avoid the low-velocity region of phase-space, preferring the intense ram-pressure stripping areas. In other words, many of the jellyfish galaxies that sit outside the high-intensity ram-pressure stripping zone in Fig. 8 are possibly being affected by substructures within the cluster and clumpy ICM. As mentioned earlier, we plan to present an in-depth analysis of the presence and effect of cluster substructure in the formation of jellyfish galaxies in a follow-up study. Lastly, it is also possible that some of these galaxies, although are clearly being disturbed by ram pressure, are not well represented by our models, or have not lost a significant fraction of gas ($>$ 10 per cent) to the ICM yet.

If we group all stripping cases together ('Extreme stripping', 'Stripping' and 'Post-stripping'), ∼60 per cent are inside or very near the plotted ram-pressure stripping 'cones'. The lowest coincidence occurs for low-mass galaxies in low-mass clusters. Finally, many of the galaxies classified as 'Unknown' are also located inside or near this region, which suggests that ram pressure could be at least one of the mechanisms responsible for their disturbed appearance.

Overall, the properties of the jellyfish galaxies, as revealed from MUSE data, together with their location in position versus velocity phase-space conclusively show that ram-pressure stripping by the dense ICM is the main mechanism responsible for the jellyfish-like features in these galaxies. Moreover, our results support a scenario in which ram pressure incrementally strips the gas from galaxies, with peak-stripping occurring as they approach pericentre. Our findings

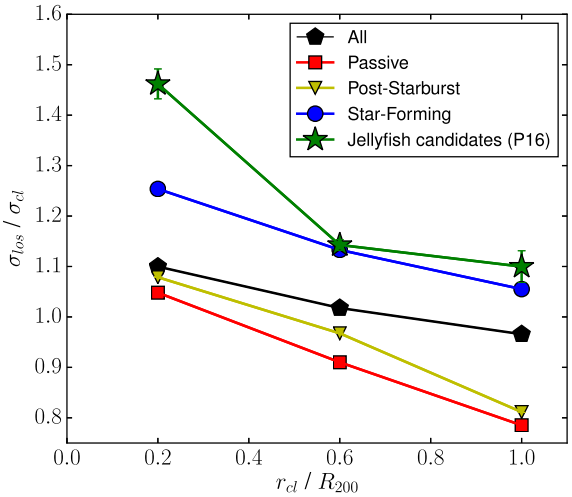

Figure 9. Line-of-sight cluster velocity dispersion radial profiles of all the cluster jellyfish candidates from P16, and the samples of passive, star-forming, and post-starburst galaxies from Paccagnella et al. (2017), normalized by the velocity dispersion of the cluster as a function of distance from the cluster centre in units of R_{200}. The parent sample of WINGS/OmegaWINGS cluster galaxies is plotted in black for reference. We considered all candidate jellyfish (which include the confirmed cases from GASP) and did not differentiate by class to increase the number of galaxies per radial bin. Errors are jackknife standard deviations. For this plot we restricted the galaxy samples to the clusters with spectroscopic completeness $>$ 50 per cent and cluster-centric distances $r_{\rm cl} < R_{200}$ to minimize biases.

are in agreement with the HI-stripping sequence presented in Yoon et al. (2017).

4.2 Cluster velocity dispersion

Additional information about the orbits of cluster galaxies may also be retrieved from the cluster velocity dispersion of different galaxy populations as a function of projected cluster-centric distance (see e.g Biviano & Katgert 2004; Haines et al. 2015). In Fig. 9, the cluster velocity dispersion of the jellyfish galaxies (green stars) is compared with other galaxy populations defined in the following. We use here the spectral classification of WINGS/OmegaWINGS galaxies presented in Paccagnella et al. (2017), who defined 'star-forming' galaxies as those with Hα or other emission lines in their spectra, and separated the galaxies without emission into 'Passive' and 'Post-starburst'. The 'Passive' type has weak Hδ in absorption (Hδ $<$ 3Å, typical of K-type stars), while the 'Post-starburst' displays a combination of signatures typical of both K- and A-type stars with strong Hδ in absorption (Hδ $>$ 3 A).

In Fig. 9, the red line with the lowest cluster velocity dispersion at all clustercentric radii corresponds to the passive galaxies, and mostly traces the oldest population of cluster galaxies. The low-velocity dispersion of these galaxies indicates they have 'virialized' or settled into the cluster potential. The blue line corresponds to star-forming galaxies that typically trace galaxies that have not been in the cluster for more than one or two pericentric passages, which explains the higher cluster velocity dispersion, typical of non-virialized cluster members. Now, if we separate the jellyfish galaxy candidates (of all classes) from the rest of the parent star-forming population we get the green line, which shows a dramatic increase of cluster velocity dispersion at low radii. In fact, the KS probability that the phase-space distribution of jellyfish candidates is drawn from the same distribution as star-forming galaxies (at

Downloaded from https://academic.oup.com/mnras/article/476/4/4753/4904145 by CIS Psicologia Biblioteca F.Metelli - Universita degli Studi di Padova user on 14 October 2020

$r_{cl} < R_{200}$) is very low (0.001 per cent). Assuming that the star-forming galaxies are the progenitors of jellyfish, the steep radial cluster velocity dispersion profile of jellyfish can be explained by highly radial orbits, and is consistent with the required conditions for ram-pressure stripping, which peaks near first pericentre. Moreover, the velocity distribution of our jellyfish galaxies is consistent with the steep cluster velocity dispersion profile of H I-deficient galaxies (Solanes et al. 2001). Our results are also consistent with the work by Vulcani et al. (2017), who studied the orbits of potentially ram-pressure stripped galaxies in intermediate-redshift clusters, selected to have offsets in the the peak of H α emission with respect to UV continuum. Using cosmological simulations as referece (Jiang et al. 2015), they concluded that stripped galaxies are on first infall, and consist of the 25 per cent most radial orbits.

It is interesting to include the post-starburst galaxies in the comparison. Fig. 9 shows that their cluster velocity dispersion profile (yellow line) is slightly above the passive galaxies. This was already seen in Paccagnella et al. (2017), who concluded that the post-starburst galaxy population arises from a fast shut-off of the star formation that changes the spectral features of the galaxy before it changes its colour and morphology (see also Poggianti et al. 2004; Muzzin et al. 2014). Considering the fast-acting effect of ram-pressure stripping it is likely that post-starburst galaxies experienced significant gas stripping prior to obtaining post-starburst features. We will further investigate this idea in forthcoming papers by analysing the post-starburst galaxies in the GASP sample.

5 SUMMARY AND CONCLUSIONS

In this paper we have presented the first large study of the orbital histories of jellyfish galaxies in clusters, utilizing the vast spectroscopic sample of cluster galaxies from the WINGS and OmegaWINGS surveys, the associated catalogue of jellyfish candidates from P16, and the subset of confirmed jellyfish galaxies observed with MUSE by the ongoing GASP survey (Poggianti et al. 2017b). We list our main findings below.

(i) We first characterize the sample of confirmed and candidate jellyfish galaxies and the control sample of non-stripped galaxies, which display a broad range of stellar mass and cluster mass. Jellyfish galaxies observed by MUSE were classified according to their H α morphology. The classification yielded four broad categories related to their apparent gas stripping stage: 'Stripping' (one-sided asymmetries of the gas), 'Extreme-stripping' (tails of stripped gas longer than the stellar body of the galaxy), 'Post-stripping' (truncated H α profiles relative to the stellar disc) and '?' (unclear asymmetry).

(ii) Using the parent sample of WINGS/OmegaWINGS clusters as reference, we constructed an analytic model of the ICM in two extreme cases: a low-mass cluster (Virgo, Cluster A) and a high mass cluster (A85, Cluster B). Similarly, we took an average low mass ($10^{9.6} M_{\odot}$, Galaxy I) and a high mass galaxy ($10^{10.7} M_{\odot}$, Galaxy II) from our sample to build two realistic models of the radial profile of the anchoring force in each case. By comparing the galaxy models with the cluster models, it is possible to study the effect of ram pressure in different scenarios. In particular, we provide the *recipe for tracing ram-pressure intensity in position versus velocity phase-space diagrams of galaxies in clusters, and estimate the amount of total mass stripped from infalling galaxies.*

(iii) We then utilize phase-space diagrams as diagnostic tool to infer the orbital histories of the cluster galaxies and the intensity of ram-pressure stripping exerted by the ICM. We find that:

(a) The distribution of jellyfish galaxy candidates in phase-space spans a broad range of projected cluster-centric distances, but is preferentially shifted towards higher absolute line-of-sight velocities than the overall population of cluster galaxies at all cluster-centric radii. This suggests that *jellyfish galaxies were recently accreted into the clusters*.

(b) When separating the confirmed jellyfish galaxies observed by GASP we find that the distribution of 'Stripping', 'Extreme-stripping' and 'Post-stripping' galaxies is consistent with *incremental outside-in gas stripping of infalling galaxies*. The vicinity of the most extreme jellyfish to the cluster centre suggests that they are undergoing peak stripping near pericentre. Interestingly all the 'Extreme stripping' galaxies have stellar masses $>10^{10} M_{\odot}$.

(c) Finally, jellyfish galaxies show a steeper cluster velocity dispersion (especially at low projected cluster-centric distances) than passive and even star-forming galaxies, which indicates that *they are preferentially on radial orbits*.

Overall, our results reveal that jellyfish galaxies are a population of recently accreted cluster galaxies on highly radial orbits, that are stripped via ram pressure as they pass through the dense cluster core at very high speeds. Since we detect significant gas stripping on first infall, we conclude that the theoretical prediction that gas removal is a fast ($\sim$1–2 Gyr; first pericentric passage) and incremental outside-in effect driven by the ICM. This is consistent with the stripping time-scale found in cosmological simulations of cluster galaxies ($\gtrsim$1 Gy; Tonnesen, Bryan & van Gorkom 2007) and the free-fall time of a galaxy moving from $1.5 \times R_{200}$ to $0.25 \times R_{200}$ (1.1 Gry). The most spectacular jellyfish galaxies in our sample are high-mass galaxies located close to the cluster core (in projection). Simulations of ram-pressure stripping suggests that the observed long tails of ionized stripped gas are only possible to form under the most intense ram-pressure conditions. It is thus possible that only the massive galaxies were able to still have gas by the time they reached the vicinity of the cluster core and thus are the only ones displaying long bright tails.

The characterization of ram-pressure stripping in phase-space based on the cluster and galaxy models presented in Section 3 can serve as a reference for other ram-pressure stripping studies (including published and future GASP papers). Although these models are simplistic and idealized, they have proven to be very good at predicting the amount of stripping for disc galaxies infalling into relatively regular galaxy clusters. In fact, the results presented in this paper are supported by cosmological (Oman et al. 2013; Haines et al. 2015; Jaffé et al. 2015; Rhee et al. 2017) and hydrodynamical simulations (e.g. Roediger & Brüggen 2006; Tonnesen & Bryan 2009; Steinhauser et al. 2016), as well as similar studies of the distribution of H I-deficient and non-deficient galaxies in nearby clusters (Solanes et al. 2001; Yoon et al. 2017). The known uncertainties in our ram-pressure stripping modelling introduced by the use of projected phase-space diagrams can be overcome when working with statistically large samples of galaxies.

Finally, it is important to note that the results presented in this paper are based on a sample of mostly relaxed clusters. There is evidence however that in dynamically disturbed clusters extreme ram-pressure stripping events can be abundant (Vijayaraghavan & Ricker 2013; Jaffé et al. 2016; McPartland et al. 2016). It is reasonable to conclude that in a hierarchical Universe, the conditions where extreme ram-pressure stripping occurs depend not only on the properties of the galaxy, mass of the host cluster, and orbital parameters (as described in this paper), but also on the dynamical state of the host cluster/group. We plan to present a dedicated study

Downloaded from https://academic.oup.com/mnras/article/476/4/4753/4904145 by CIS Psicologia Biblioteca F.Metelli - Universita degli Studi di Padova user on 14 October 2020

of the effect of cluster sub-structuring in the formation of jellyfish galaxies in a future publication.

ACKNOWLEDGEMENTS

Based on observations collected at the European Organization for Astronomical Research in the Southern hemisphere under ESO programme 196.B-0578. We thank Jinsu Rhee for providing the simulations data used in this paper and Graeme Candlish and Chris Haines for useful discussions. We acknowledge financial support from PRIN-SKA 2017 (PI Hunt). B.V. acknowledges the support from an Australian Research Council Discovery Early Career Researcher Award (PD0028506).

REFERENCES

Abadi M. G., Moore B., Bower R. G., 1999, MNRAS, 308, 947
Aguerri J. A. L., Agulli I., Diaferio A., Dalla Vecchia C., 2017, MNRAS, 468, 364
Barnes J. E., Hernquist L., 1996, ApJ, 471, 115
Bellhouse C. et al., 2017, ApJ, 844, 49
Biviano A., Katgert P., 2004, A&A, 424, 779
Biviano A., Katgert P., Mazure A., Moles M., den Hartog R., Perea J., Focardi P., 1997, A&A, 321, 84
Boselli A., Gavazzi G., 2006, PASP, 118, 517
Boselli A., Gavazzi G., 2014, A&A Rev., 22, 74
Boselli A et al., 2011, A&A, 528, A107
Bravo-Alfaro H., Caretta C. A., Lobo C., Durret F., Scott T., 2009, A&A, 495, 379
Byrd G., Valtonen M., 1990, ApJ, 350, 89
Calvi R., Poggianti B. M., Vulcani B., 2011, MNRAS, 416, 727
Cava A. et al., 2009, A&A, 495, 707
Cavaliere A., Fusco-Femiano R., 1976, A&A, 49, 137
Cayatte V., van Gorkom J. H., Balkowski C., Kotanyi C., 1990, AJ, 100, 604
Cayatte V., Kotanyi C., Balkowski C., van Gorkom J. H., 1994, AJ, 107, 1003
Chabrier G., 2003, PASP, 115, 763
Chen Y., Reiprich T. H., Böhringer H., Ikebe Y., Zhang Y.-Y., 2007, A&A, 466, 805
Chung A., van Gorkom J. H., Kenney J. D. P., Crowl H., Vollmer B., 2009, AJ, 138, 1741
Colless M., Dunn A. M., 1996, ApJ, 458, 435
Cowie L. L., Songaila A., 1977, Nature, 266, 501
D'Onofrio M. et al., 2014, A&A, 572, A87
Durret F., Lima Neto G. B., Forman W., 2005, A&A, 432, 809
Ebeling H., Voges W., Bohringer H., Edge A. C., Huchra J. P., Briel U. G., 1996, MNRAS, 281, 799
Ebeling H., Edge A. C., Bohringer H., Allen S. W., Crawford C. S., Fabian A. C., Voges W., Huchra J. P., 1998, MNRAS, 301, 881
Ebeling H., Edge A. C., Allen S. W., Crawford C. S., Fabian A. C., Huchra J. P., 2000, MNRAS, 318, 333
Ebeling H., Stephenson L. N., Edge A. C., 2014, ApJ, 781, L40
Fasano G. et al., 2006, A&A, 445, 805
Fasano G. et al., 2012, MNRAS, 420, 926
Ferrarese L. et al., 2012, ApJS, 200, 4
Fossati M., Fumagalli M., Boselli A., Gavazzi G., Sun M., Wilman D. J., 2016, MNRAS, 455, 2028,
Fritz J. et al., 2007, A&A, 470, 137
Fritz J. et al., 2011, A&A, 526, A45
Fritz J. et al., 2014, A&A, 566, A32
Fritz J. et al., 2017, ArXiv e-prints
Fumagalli M., Fossati M., Hau G. K. T., Gavazzi G., Bower R., Sun M., Boselli A., 2014, MNRAS, 445, 4335
Gullieuszik M. et al., 2015, A&A, 581, A41
Gullieuszik M. et al., 2017, ApJ, 846, 27
Gunn J. E., Gott J. R. I., 1972, ApJ, 176, 1
Haines C. P. et al., 2015, ApJ, 806, 101
Haynes M. P., Giovanelli R., Chincarini G. L., 1984, ARA&A, 22, 445
Hernández-Fernández J. D., Haines C. P., Diaferio A., Iglesias-Páramo J., Mendes de Oliveira C., Vilchez J. M., 2014, MNRAS, 438, 2186
Hernquist L., 1990, ApJ, 356, 359
Hess K. M., Wilcots E. M., 2013, AJ, 146, 124
Jaffé Y. L., Poggianti B. M., Verheijen M. A. W., Deshev B. Z., van Gorkom J. H., 2012, ApJ, 756, L28
Jaffé Y. L., Smith R., Candlish G. N., Poggianti B. M., Sheen Y.-K., Verheijen M. A. W., 2015, MNRAS, 448, 1715
Jaffé Y. L. et al., 2016, MNRAS, 461, 1202
Jiang L., Cole S., Sawala T., Frenk C. S., 2015, MNRAS, 448, 1674
Kempner J. C., Sarazin C. L., Ricker P. M., 2002, ApJ, 579, 236
Kenney J. D. P., Koopmann R. A., 1999, AJ, 117, 181
Kenney J. D. P., van Gorkom J. H., Vollmer B., 2004, AJ, 127, 3361
Kenney J. D. P., Geha M., Jáchym P., Crowl H. H., Dague W., Chung A., van Gorkom J., Vollmer B., 2014, ApJ, 780, 119
Mahajan S., Mamon G. A., Raychaudhury S., 2011, MNRAS, 416, 2882
McLaughlin D. E., 1999, ApJ, 512, L9
McPartland C., Ebeling H., Roediger E., Blumenthal K., 2016, MNRAS, 455, 2994
Mei S. et al., 2007, ApJ, 655, 144
Merluzzi P. et al., 2013, MNRAS, 429, 1747
Mohr J. J., Geller M. J., Wegner G., 1996, AJ, 112, 1816
Moore B., Katz N., Lake G., Dressler A., Oemler A., 1996, Nature, 379, 613
Moretti A. et al., 2014, A&A, 564, A138
Moretti A. et al., 2018, MNRAS, 475, 4055
Muzzin A. et al., 2014, ApJ, 796, 65
Navarro J. F., Frenk C. S., White S. D. M., 1996, ApJ, 462, 563
Nulsen P. E. J., 1982, MNRAS, 198, 1007
Oman K. A., Hudson M. J., 2016, MNRAS, 463, 3083
Oman K. A., Hudson M. J., Behroozi P. S., 2013, MNRAS, 431, 2307
Owers M. S., Couch W. J., Nulsen P. E. J., Randall S. W., 2012, ApJ, 750, L23
Paccagnella A. et al., 2017, ApJ, 838, 148
Pignatelli E., Fasano G., Cassata P., 2006, A&A, 446, 373
Poggianti B. M., Bridges T. J., Komiyama Y., Yagi M., Carter D., Mobasher B., Okamura S., Kashikawa N., 2004, ApJ, 601, 197
Poggianti B. M. et al., 2016, AJ, 151, 78
Poggianti B. M. et al., 2017a, Nature, 548, 304
Poggianti B. M. et al., 2017b, ApJ, 844, 48
Popping G., Somerville R. S., Trager S. C., 2014, MNRAS, 442, 2398
Rasmussen J., Ponman T. J., Mulchaey J. S., 2006, MNRAS, 370, 453
Rasmussen J., Ponman T. J., Verdes-Montenegro L., Yun M. S., Borthakur S., 2008, MNRAS, 388, 1245
Rawle T. D. et al., 2014, MNRAS, 442, 196
Rhee J., Smith R., Choi H., Yi S. K., Jaffé Y. L., Candlish G. N., Sanchez-Janssen R., 2017, ApJ, 843, 128
Roediger E., Brüggen M., 2006, MNRAS, 369, 567
Sheen Y.-K. et al., 2017, ApJ, 840, L7
Solanes J. M., Manrique A., García-Gómez C., González-Casado G., Giovanelli R., Haynes M. P., 2001, ApJ, 548, 97
Steinhauser D., Schindler S., Springel V., 2016, A&A, 591, A51
Tonnesen S., Bryan G. L., 2009, ApJ, 694, 789
Tonnesen S., Bryan G. L., 2012, MNRAS, 422, 1609
Tonnesen S., Bryan G. L., van Gorkom J. H., 2007, ApJ, 671, 1434
Varela J. et al., 2009, A&A, 497, 667
Verdes-Montenegro L., Yun M. S., Williams B. A., Huchtmeier W. K., Del Olmo A., Perea J., 2001, A&A, 377, 812
Vijayaraghavan R., Ricker P. M., 2013, MNRAS, 435, 2713
Vollmer B., Cayatte V., Balkowski C., Duschl W. J., 2001, ApJ, 561, 708
Vulcani B. et al., 2017, ApJ, 837, 126
Yoon H., Chung A., Smith R., Jaffé Y. L., 2017, ApJ, 838, 81
Yoshida M. et al., 2008, ApJ, 688, 918

This paper has been typeset from a TEX/LATEX file prepared by the author.

Downloaded from https://academic.oup.com/mnras/article/476/4/4753/4904145 by CIS Psicologia Biblioteca F.Metelli - Universita degli Studi di Padova user on 14 October 2020